Ann Microbiol (2015) 65:411–421
DOI 10.1007/s13213-014-0874-3

ORIGINAL ARTICLE

Exploring strategies for adsorption of azo dye Congo Red using free and immobilized biomasses of *Trametes pubescens*

Jing Si · Tong-Qi Yuan · Bao-Kai Cui

Received: 10 November 2013 / Accepted: 10 March 2014 / Published online: 30 March 2014

Abstract Immobilized biomass of white rot fungus *Trametes pubescens* was explored for adsorption of azo dye Congo Red. The biomass immobilized by sodium alginate enhanced the sorption capacity for Congo Red approximately 4-fold of the free biomass, which competed well with other reported sorbents. Dye uptake was favored by acidic conditions at pH 2.0 with increasing initial dye concentration up to 100 mg/L using less biomass at room temperature and agitation speed. Adsorption of dyes onto the biomass was weakly dependent on ionic strength. Additionally, the adsorption process followed the pseudo-second-order kinetic and Freundlich isotherm models. During this process, the morphological changes on the biomass surface occurred; the amine functional groups present on the cell surface were mainly responsible for this process, and reduction in crystallinity of the biomass was observed, as confirmed by SEM, FT-IR, and X-ray diffraction, respectively. Desorption experiments were performed to regenerate the sorbent, making the process more economic and environmentally friendly. These demonstrated that the immobilized *T. pubescens* biomass is a promising sorbent for Congo Red removal.

Keywords Dye adsorption · *Trametes pubescens* biomass · Immobilization · Kinetic modeling · Adsorption isotherms

J. Si · B.-K. Cui (✉)
Institute of Microbiology, Beijing Forestry University, P.O. Box 61, Qinghuadong Road 35, Haidian District, Beijing 100083, People's Republic of China
e-mail: baokaicui2013@gmail.com

T.-Q. Yuan
Beijing Key Laboratory of Lignocellulosic Chemistry, Beijing Forestry University, Beijing 100083, People's Republic of China

Introduction

Since 1856, when the first synthetic dye was reported, the commercial use of dyes has greatly increased as the number of textile synthetic dyes used today exceeds 1×10^5 (Hosseini Koupaie et al. 2012). Azo dyes are among the largest and most versatile class with the greatest variety of colors, having wide applications in textile, food, plastics, pharmaceuticals, cosmetics, paper printing, leather, and other industries (Anjaneya et al. 2011). Approximately half a million tons of them are produced every year all over the world and account for two-thirds of the total dyestuff market (Zhang et al. 2012). Unfortunately, during textile procedures, inefficiencies in dyeing result in large amounts of dyestuff being directly lost into the wastewater, which ultimately finds its way into the environment (Zeng et al. 2011). Effluents from the textile industries containing dyes are highly colored, which reduces the amount of sunlight to photosynthetic organisms, resulting in decreased oxygen levels and deteriorative water qualities in aquatic ecosystems (Champagne and Ramsay 2010). Moreover, many of the azo dyes and/or their breakdown products from effluents have been shown to be toxic, potentially carcinogenic, and can lead to the formation of bladder cancer in humans, tumors, allergies, nuclear anomalies in experimental animals, and chromosomal aberrations in mammalian cells (Mendes et al. 2011). Unless the wastewater is properly treated, these dyes may significantly lead to severe contamination of both surface and ground water.

Recently, studies on treatment of textile effluents have mainly been centered on the development of an efficient and cost-effective removal process (Shah et al. 2012). As dyes are designed to be resist fading upon exposure to sweat, light, water, many chemicals including agents, and microbial attack, dye-containing effluents are little decolorized by conventional physical, chemical, and biological wastewater treatments, including adsorption, chemical coagulation, precipitation,

filtration, electro dialysis, membrane separation, oxidation, and so on (Pathak et al. 2011). Furthermore, some of these technologies are limited because of the excessive usage of chemicals, accumulation of concentrated sludge, expensive materials requirements, and high operational costs (Xiong et al. 2010).

Biosorption is an attractive technology in terms of flexibility, water reuse, waste recovery, simplicity of design, ease of operation, and insensitivity to toxic pollutants (Yang and Feng 2010). It can be defined as a number of metabolism-independent processes (physical and chemical adsorption, ion exchange, complexation, chelation, and micro-precipitation) taking place essentially in the cell wall of the live or dead biomass or their derivatives (Aksu 2005). This biomass may be bacteria, fungi, algae from biological wastewater treatment plants, and by-products from fermentation industries or seaweeds. Textile dyes vary greatly in their chemistries, and their interactions with microorganisms depend on the chemistry of a particular dye, type of biomass, its preparation, and its specific surface properties and environmental conditions (pH, temperature, ionic strength, existence of competing organic or inorganic ligands in solution) (Vijayaraghavan and Yun 2008). Recently, numerous approaches have been studied for the development of cheap and effective adsorbents. The performance of adsorbent is usually the key influence on adsorption. Moreover, the adsorption capacities of adsorbents mainly depend on various characteristics such as surface area, pore structure, and loaded functional groups (Wang et al. 2010). Unlike conventional sorbents, fungal biomass used as sorbent does not generate huge quantities of sludge and, due to its genetic diversity, metabolic versatility, and widespread occurrence, it is emerging as a viable alternative to remediate pollution problems caused by dyes (Xin et al. 2012).

Aspergillus niger, *Funalia trogii*, *Ganoderma applanatum*, *Neurospora crassa*, *Phanerochaete chrysosporium*, *Rhizopus stolonifer*, *Trametes pubescens*, *Trametes versicolor*, and so on are the some low-cost fungal biomasses which have been used as sorbents for dye removal (Fu and Viraraghavan 2001; Aksu 2005; Bayramoğlu et al. 2006; Xiong et al. 2010). Among these fungi, *T. pubescens* is one of the most widespread fungi in China (Dai 2012), and recent studies showed that active *T. pubescens* exhibits excellent decolorization capability in removing various synthetic dyes (Si and Cui 2013; Si et al. 2013a, b). Moreover, the presence of potentially toxic compounds in the culture of *T. pubescens* did not inhibit fungal growth and decolorization capacity, and could also be useful as the energy source. However, there are few reports on the adsorption of textile dyes by *T. pubescens*, which is inexpensive, easily growth, readily available, and produces high yields of biomass.

In the present study, the biomass from *T. pubescens* after its immobilization was utilized as a sorbent for removal of azo dye Congo Red. The major objective was to achieve the maximum adsorption efficiency of the dye by optimizing the interacting process factors, i.e. initial solution pH, initial dye concentration, and ionic strength. Additionally, adsorption kinetic data of the biomass were tested by the Lagergren first-order, pseudo-second-order, and intraparticle diffusion models. Equilibrium behavior was analyzed based on the Langmuir, Freundlich, and Temkin adsorption isotherms. Scanning electron microscope (SEM), fourier transform-infrared spectroscopy (FT-IR), and X-ray diffraction (XRD) studies were carried out to understand the surface properties of the biomass involved in the adsorption process.

Materials and methods

Adsorbate and chemicals

In this study, azo dye Congo Red (chemical formula: $C_{32}H_{22}N_6Na_2O_6S_2$, color index number: 22120, color index name: Direct Red 28, chromophore: disazo, molecular weight: 696.68 g/mol, λ_{max}=488 nm) was prepared by being filtered through a 0.22-μm membrane to remove bacteria before use. Agar powder, 2,2′-azino-bis(3-ethylbenzthiazoline-6-sulphonic acid) (ABTS), sodium alginate, and D201 were all Sigma-Aldrich products (St. Louis, MO, USA). All the reagents used were of analytical grade.

Biomass preparation

The fungal strain *T. pubescens* BJFC 006059 was isolated from Chebaling Nature Reserve of Guangdong Province in China. It was maintained through periodic (monthly) transfer on yeast extract glucose agar (YGA) at 4 °C. The YGA medium contained (g/L of distilled water): yeast extract 5, glucose 20, agar 20, KH_2PO_4 1, $MgSO_4 \cdot 7H_2O$ 0.5, $ZnSO_4 \cdot 7H_2O$ 0.05, and vitamin B1 0.01, and the pH of the medium was adjusted to 5.0 before sterilization. Prior to use, the stored fungal strain was activated in 100 mL of yeast extract glucose medium (YG; identical to YGA without agar) and cultured on a rotary shaker at 28 °C with a speed of 150 rpm. After 6 days, mycelium was homogenized using an Ace Homogenizer (Hengao, Tianjin, China) at 5,000 rpm for 30 s, and the pellet suspension was later prepared as inoculum for the next experiment.

An aliquot of 10 mL of inoculum (0.087 g, dry weight) was inoculated into a 250-mL Erlenmeyer flask containing 100 mL of YG medium, and incubated at 28 °C and 150 rpm. After 5 days, the biomass was then harvested by filtration, washed, oven-dried at 75 °C for 24 h, powdered (< 75 μm), and immobilized by suspending 0.1 g dry weight of the biomass in 5 mL of double-distilled water, mixed with 4 % (w/v) sodium alginate solution or 4 % (v/v) D201, and

dropped into 0.5 M calcium chloride ($CaCl_2$) solution using a syringe when the biomass beads (3.0±0.1 mm diameter) were formed. The beads entrapping the fungal biomass were kept overnight at 4 °C in $CaCl_2$ solution (0.5 M) followed by repeated washing with double-distilled water and stored at 4 °C in distilled water prior to their use as the sorbents.

Batch adsorption studies

Batch adsorption studies were conducted by adding 50 mg of free or immobilized biomass to 250-mL Erlenmeyer flasks containing 100 mL of dye solution (100 mg/L) and shaken on a rotary shaker for 60 min with agitation speed of 150 rpm at 28 °C. The influences of different factors such as initial solution pH (1.0–10.0), initial dye concentration (25–200 mg/L), and ionic strength (NaCl, 0.5 %–5.0 %, w/v) were evaluated to achieve the maximum adsorption efficiency by varying the factor under study and keeping other factors constant. Control experiments were also performed without addition of biomass to confirm that the adsorption of the dye onto conical flasks was negligible. All adsorption experiments were performed in triplicate. A two-way analysis of variance (ANOVA) was performed on the adsorption capacity data to distinguish statistical differences ($P<0.01$) among the interacting process factors with free and immobilized *T. pubescens* biomasses. All statistical analyses were performed by using SPSS 20.0 software. The superscript letters in Table 1 represent the ANOVA results.

The cultures harvested at different time intervals were centrifuged at 12,000 rpm for 20 min, and the cell-free supernatant was used for enzyme assay. All the enzyme activities were monitored spectrophotometrically at room temperature where reference blanks contained all components except the enzyme solution. Laccase activity was determined by measuring the oxidation of 1 mM ABTS at 420 nm (Daneshvar et al. 2007). Lignin peroxidase activity was determined by monitoring the formation of propanaldehyde at 300 nm (Parshetti et al. 2006).

Table 1 Influences of interacting process factors on the adsorption capacities of free and immobilized *Trametes pubescens* biomasses for azo dye Congo Red

Factor	Level	Adsorption capacity (mg/g)		
		Free biomass	Alginate-immobilized biomass	D201-immobilized biomass
Initial solution pH	1.0	68.25 ± 2.57^{B}	355.48 ± 5.04^{C}	154.21 ± 0.93^{D}
	2.0	77.18 ± 0.95^{A}	380.56 ± 0.63^{A}	176.54 ± 0.77^{A}
	3.0	70.05 ± 1.19^{B}	371.26 ± 1.07^{B}	171.41 ± 1.13^{B}
	4.0	57.15 ± 1.30^{C}	343.15 ± 2.03^{D}	160.24 ± 2.33^{C}
	5.0	51.64 ± 1.24^{D}	281.43 ± 3.01^{E}	117.42 ± 2.34^{E}
	6.0	33.39 ± 0.40^{E}	233.34 ± 1.46^{F}	87.25 ± 0.90^{F}
	7.0	30.33 ± 0.18^{F}	121.45 ± 1.12^{G}	65.13 ± 1.72^{G}
	8.0	28.48 ± 2.36^{F}	87.12 ± 1.55^{H}	45.21 ± 1.01^{I}
	9.0	21.44 ± 1.14^{G}	66.23 ± 0.99^{I}	51.10 ± 2.83^{H}
	10.0	19.23 ± 0.92^{G}	30.20 ± 2.86^{J}	44.15 ± 1.28^{I}
Initial dye concentration (mg/L)	25	34.17 ± 0.83^{H}	156.51 ± 4.66^{H}	42.10 ± 2.02^{H}
	50	77.18 ± 1.09^{F}	377.56 ± 6.97^{F}	176.54 ± 2.64^{E}
	60	91.32 ± 1.32^{D}	411.15 ± 1.52^{D}	212.26 ± 1.23^{C}
	80	118.50 ± 2.35^{C}	465.32 ± 0.99^{C}	238.81 ± 1.20^{B}
	100	125.05 ± 0.75^{A}	495.24 ± 1.76^{A}	248.81 ± 3.22^{A}
	120	122.32 ± 1.40^{B}	483.36 ± 1.66^{B}	235.51 ± 2.14^{B}
	150	87.71 ± 1.39^{E}	402.37 ± 2.22^{E}	206.40 ± 2.85^{D}
	180	62.05 ± 1.12^{G}	282.21 ± 2.85^{G}	144.49 ± 2.50^{F}
	200	28.19 ± 1.01^{I}	135.38 ± 0.88^{I}	97.08 ± 1.59^{G}
Ionic strength (NaCl, %, w/v)	0	125.05 ± 1.26^{E}	495.24 ± 1.27^{E}	248.81 ± 3.24^{C}
	0.5	129.12 ± 2.49^{D}	507.74 ± 0.41^{D}	251.12 ± 1.27^{C}
	1.0	135.35 ± 1.38^{B}	531.52 ± 0.69^{C}	258.32 ± 2.33^{B}
	1.5	138.56 ± 1.11^{A}	548.19 ± 2.43^{A}	265.12 ± 0.99^{A}
	2.0	132.21 ± 1.09^{C}	534.51 ± 1.62^{B}	256.67 ± 0.57^{B}
	3.0	115.54 ± 0.68^{F}	507.84 ± 2.52^{D}	241.28 ± 2.11^{D}
	4.0	104.47 ± 1.24^{G}	456.65 ± 0.66^{F}	212.24 ± 1.68^{E}
	5.0	87.74 ± 0.43^{H}	348.82 ± 1.21^{G}	181.20 ± 1.80^{F}

The superscript letters indicate ANOVA results. The same letter denotes that the difference between two treatments is not statistically significant. Otherwise, the difference is statistically significant ($P<0.01$)

After equilibrium, the solution was filtered and the filtrates were subsequently analyzed for residual dye concentration with a UV-visible spectrophotometer (UNICO 4802; Younike, Shanghai, China). The dye removal efficiency (%) and the amount of dye adsorbed on the biomass (q_e) were calculated by Eqs. 1 and 2 as follows:

$$\text{Dye removal efficiency}(\%) = \frac{C_i - C_e}{C_i} \ldots\ldots \quad (1)$$

$$q_e = \frac{V(C_i - C_e)}{m} \ldots\ldots \quad (2)$$

where C_i and C_e are the initial and equilibrium concentrations (mg/L) of azo dye Congo Red, q_e is the dye uptake (mg/g), V is the solution volume (L), and m is the mass of biomass (g).

Kinetic rate constants were determined using Lagergren first-order, pseudo-second-order and intraparticle diffusion models. Adsorption data were subject to equilibrium modeling to have a better understanding of adsorption of Congo Red dye using isotherms such as Langmuir, Freundlich, and Temkin.

The dye loaded biomass (50 mg) was desorbed with 100 mL of 0.1 M sodium hydroxide (NaOH) for 60 min. Subsequently, the dye desorbed biomass was washed and the same biomass was used in three sorption–desorption cycles to regenerate the spent biomass beads.

Adsorption characterization

The surface morphological changes of the free and immobilized biomasses before and after adsorption of Congo Red dye was explored by SEM. FT-IR technique was used to examine the surface functional groups responsible for dyes adsorption. XRD was carried out to verify the crystalline or amorphous structures of the free and immobilized biomasses before and after dye loading. These tests were conducted following the procedures obtained by Dotto et al. (2012).

Results and discussion

Influence of initial solution pH

Initial solution pH significantly influences the overall adsorption process. It affects not only surface charge, degree of ionization, and dissociation of functional groups on the active sites of sorbent but also structure of dye molecule (Crini et al. 2007). The data of dye uptake versus pH are shown in Fig. 1a and Table 1. Little adsorption took place at the initial pH range of 5.0–10.0. The decrease in dye uptake with increasing initial solution pH may be attributed to the successive deprotonation of positively charged groups on sorbents and electrostatic

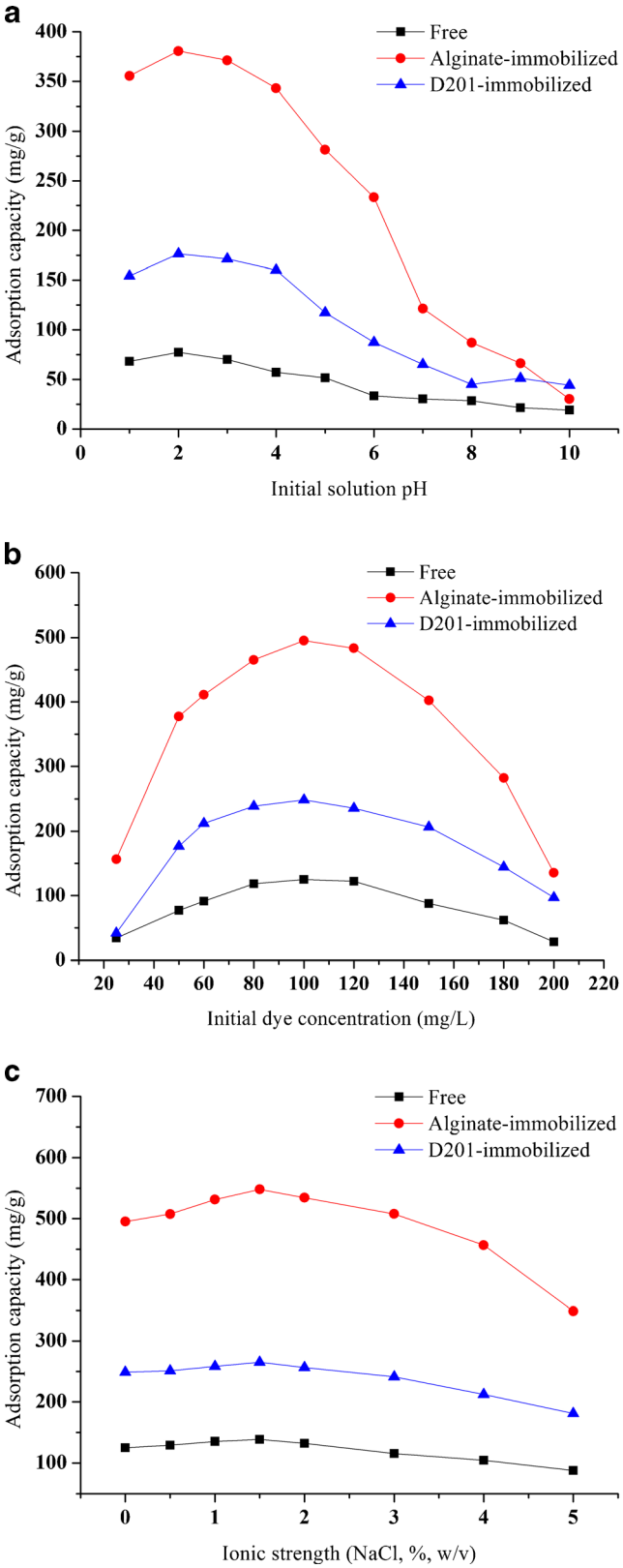

Fig. 1 Influences of initial solution pH (**a**), initial dye concentration (**b**), and ionic strength (**c**) on adsorption of azo dye Congo Red onto free and immobilized *Trametes pubescens* biomasses

repulsion between negatively charged sites on sorbents and Congo Red dye. At high pH, a high concentration of OH^- could neutralize the positively charged surface of biomass and compete with the anionic dye molecule for the adsorption sites (Çolak et al. 2009). Moreover, adsorption capacity of Congo Red dye increased with decreasing the initial solution pH from 5.0 to 2.0, and maximum adsorption was obtained at pH 2.0 for immobilized and free biomasses. The better adsorption yield observed at lower solution pH conditions for all biomasses can be explained by the attractive forces between the anionic dyes and positively charged surface of sorbents. This may be an indicator of the strong interaction between dye and adsorbent as well as the electrostatic interaction. As the pH increases, repulsive forces between anionic dye molecules and dye binding sites of sorbent increased due to the enhancing of the negative charge density on the biomass surface. The immobilized biomass exhibited higher adsorption capacity than free biomass at all the studied pH values, which can be attributed to the modification of the biomass surface by immobilization. As maximum adsorption efficiencies of Congo Red dye for all the biomasses were observed at pH 2.0, therefore further adsorption studies were carried out at solution pH 2.0. Similar results have also been reported in the literature where the low pH was found to be favorable for anionic dyes sorption (Kousha et al. 2012). Additionally, no variations of laccase and lignin peroxidase activities were observed during the decolorization process.

Influence of initial dye concentration

Figure 1b and Table 1 depict the influence of different initial dye concentrations of Congo Red (25–200 mg/L) on the adsorption capabilities of the free and immobilized *T. pubescens* biomasses. It can be seen that adsorption of the dye at different concentrations is rapid in the initial stages and gradually decreases with the progress of adsorption until the equilibrium is reached. The dye adsorption increased from 34.17 to 125.05 mg/g onto free biomass, 156.51 to 495.24 mg/g for alginate-immobilized biomass, and 42.10 to 248.81 mg/g for D201-treated biomass by increasing the initial dye concentration from 25 to 100 mg/L. Initial concentration provides an important driving force to overcome all mass transfer resistances of the dye between the aqueous and solid phases (Khataee et al. 2010). The results suggested that treatment of biomass with immobilization increased density on the biomass surface and this facilitates electrostatic interaction between sorbents and the negatively charged anionic dyes, especially at relatively higher dye concentrations. However, all sorbents have a limited number of binding sites, which become saturated at a certain concentration. Therefore, more Congo Red dye molecules were unabsorbed in the solution due to the saturation of binding sites, leading to the decrease in the sorption capacity of biomass.

Influence of ionic strength

The wastewater containing dyes commonly has salts at a high concentration and leads to high ionic strength, which may affect the adsorption of dyes onto the adsorbent. In order to investigate the influence of inorganic salt in dye adsorption process, the experiments were carried out using 100 mg/L of initial dye solution containing various NaCl concentrations ranging from 0.5 to 5.0 % (w/v). Results in Fig. 1c and Table 1 showed that the adsorption capacity increased from 125.05 to 138.56, 495.24 to 548.19, and 248.81 to 265.12 mg/g for free, alginate-immobilized, and D201-treated biomasses, respectively, as the NaCl concentration increasing from 0 to 1.5 % (w/v). This could be explained by the influence of low-strength ionic on the activity coefficient of dye ions, which stimulates their transfer to the solid phase (Aksu and Balibek 2010). Thereafter, an increase in ionic strength exhibited a slight adverse effect on dye adsorption, which may be due to the competition between chloride anions (Cl^-) and negatively charged Congo Red dye for the same binding sites on the biomass surface. Chloride anions existing in the solution may also form complexes with the dye and therefore affect the adsorption process adversely (Sun et al. 2008). Aksu and Balibek (2010) also observed that uptake of a metal-complex anionic dye Yellow RL by dried filamentous fungus *Rhizopus arrhizus* decreased with increasing the salinity of the system. However, in the present study, adsorption of azo dye Congo Red onto the biomass was weakly dependent on ionic strength.

Kinetic modeling

Since the determination of adsorption kinetics is of great importance for predicting the control mechanism of adsorption process, a kinetic investigation was conducted. In Table 2, it was found that there was a clear difference of adsorption capacity between the experimental and calculated data, which indicated that the adsorption system did not follow the Lagergren first-order and intraparticle diffusion models. The high values of R^2 (>0.99) showed that the pseudo-second-order model was the best to represent the adsorption kinetic of Congo Red dye onto free and immobilized *T. pubescens* biomasses. This indicated that adsorption of dye onto *T. pubescens* biomass was controlled by chemiosorption, and the fungal biomass was covered by the superficial layer of dyes. Similar behavior was obtained by Dotto et al. (2012) in adsorption of food dyes acid blue 9 and food yellow 3 onto chitosan. In their work, pseudo-second-order model was also the best to represent kinetic experimental data, indicating a chemical interaction of dye-chitosan.

Adsorption isotherms

Adsorption isotherm studies give information about the distribution of adsorbate between the liquid and solid phases when

Table 2 Kinetic model constants to the adsorption of azo dye Congo Red onto free and immobilized *Trametes pubescens* biomasses in the optimal conditions

Kinetic model	Kinetic coefficient	Biomass		
		Free	Alginate-immobilized	D201-immobilized
Lagergren first-order	k_1 (1/min)	0.0367	0.0360	0.0363
	q_1 (mg/g)	152.41	602.63	294.30
	R^2	0.987	0.988	0.986
Pseudo-second-order	k_2 (g/mg·min)	0.0590	0.0628	0.0613
	q_2 (mg/g)	172.41	666.67	322.58
	R^2	0.993	0.993	0.994
Intraparticle diffusion	k_p (mg/g·min$^{1/2}$)	13.39	53.42	25.966
	C (mg/g)	27.78	103.43	48.733
	R^2	0.948	0.955	0.954

adsorption process reaches equilibrium. In the present study, the equilibrium characteristics of this adsorption were described through the Langmuir, Freundlich, and Temkin equations. Table 3 summarizes all of the isotherm model coefficients for the adsorption of Congo Red dye. It was evident from the R^2 values that the Freundlich model was more suitable for describing the adsorption of azo dye Congo Red, demonstrating further that the surfaces of *T. pubescens* biomass are heterogeneous in nature and do not possess equal distribution of binding energies on the available binding sites (Freundlich 1906). Moreover, all the 1/*n* values obtained from the Freundlich model were less than unity for free and immobilized biomasses, also indicating that adsorption of Congo Red dye onto the biomass was favorable. A comparison of maximum uptake capacities of various sorbents for azo dye Congo Red as reported in the literature is presented in Table 4. The high adsorption capacity found in this study reveals that immobilized *T. pubescens* biomass is a promising adsorbent for Congo Red removal. The differences in maximum sorption efficiencies might be due to the different structures and sorption mechanisms of various sorbents and experimental conditions.

In the present study, although the mechanisms responsible for differences of three forms of fungal biomasses were illustrated to some degree based on the analysis of adsorption/absorption space and sites, the nature of adsorption/absorption by different types of biomasses and the molecular mechanisms involved were still unknown. The dye desorption behaviors of different forms of biomasses also needed to be studied further for reuse of the sorbents.

Desorption studies

To determine the reusability of sorbents, desorption studies were repeated three times to make the treatment process more economical. The results of sorption–desorption experiments of Congo Red dye are depicted in Table 5. In the first cycle, 97.969, 97.387, and 97.455 % of the adsorbed dyes onto free, alginate-immobilized, and D201-treated biomasses, respectively, were desorbed and then the desorbed dye amounts decreased to 92.671, 94.252, and 93.191 % at the third cycle. This may be due to the small amount of biomass lost during the repeated sorption–desorption operations (Asgher and Bhatti 2010). The results showed that the

Table 3 Adsorption isotherms of azo dye Congo Red onto free and immobilized *Trametes pubescens* biomasses in the optimal conditions

Adsorption isotherm	Isotherm coefficient	Biomass		
		Free	Alginate-immobilized	D201-immobilized
Langmuir	q_{max} (mg/g)	149.25	588.24	357.14
	K_L (L/mg)	0.0522	0.0511	0.0484
	R^2	0.989	0.990	0.989
Freundlich	K_F (mg/g)	22.12	82.43	48.16
	n	2.546	2.446	2.433
	R^2	0.995	0.992	0.995
Temkin	b_T (J/mol)	82.46	20.22	34.09
	K_T (L/mg)	0.636	0.582	0.571
	R^2	0.985	0.984	0.986

Table 4 Comparison of adsorption capacities for removal of azo dye Congo Red by various sorbents reported in the literature

Sorbent	pH	q_m (mg/g)	Reference
Azadirachta indica leaf powder	6.7	128.30	Bhattacharyya and Sharma 2004
Jute stick powder	7.0	35.70	Panda et al. 2009
Pine cone	3.55	40.19	Dawood and Sen 2012
Palm kernel seed coat	6.7	66.23	Oladoja and Akinlabi 2009
Rice husk	6.0	14.00	Han et al. 2008
Sugarcane bagasse	7.0	38.20	Zhang et al. 2011
Aspergillus niger	6.0	14.72	Fu and Viraraghavan 2002
Aspergillus niger biosorbent (ANB)	6.8	357.14	Xi et al. 2013
Penicillium YW01	3.0	411.53	Yang et al. 2011
Trametes versicolor	7.0	51.81	Binupriya et al. 2008
Free *Trametes pubescens* biomass	2.0	138.56	Present work
Alginate-immobilized *T. pubescens* biomass	2.0	548.19	Present work
D201-immobilized *T. pubescens* biomass	2.0	265.12	Present work

T. pubescens biomass could be repeatedly used in the dye adsorption studies with only a slight loss in its adsorption capacity.

Adsorption characterization

In order to compare adsorption behavior of azo dye Congo Red, SEM, FT-IR, and XRD were carried out for the free and immobilized *T. pubescens* biomasses before and after the dye adsorption process. SEM is a technique to characterize the surface structure and morphology of the sorbent material. It is used to determine the particle shape and porous structure of biomass (Dotto et al. 2012). In this study, SEM photomicrographs of the free and immobilized biomasses showed the morphological changes onto the sorbent surface before and after dye loading (Fig. 2). It can be seen that the surface of unadsorbed biomass was a typically wrinkled polymeric network with considerable numbers of irregular pores. In addition, a heterogeneous surface area and porous internal structure were observed in the samples. After adsorption of Congo Red dye, biomass pores were not visible. It is suggested that a dye superficial layer has covered the entire external biomass surface.

The biomass before and after adsorption demonstrates shifting and intensification of some peaks after dye loading indicating their involvement in dye adsorption, which were interpreted based on the standard wave number (Namasivayam and Kavitha 2006). To explore the involvement of the functional groups on the cell surface in adsorption of azo dye Congo Red, free and immobilized of *T. pubescens* biomasses before and after dye loading was examined using FT-IR spectroscopy (Fig. 3). The significant band positions of the complex nature of free *T. pubescens* biomass are noted as 3,280, 2,924, 2,360, 1,628, 1,540, 1,376, and 1,032 cm^{-1}. After dye loading, the broad peak at 3280.48 cm^{-1} shifted to 3257.66 cm^{-1} suggesting overlap of –OH and −NH stretching vibrations, indicating the presence of both surface free hydroxyl groups and chemisorbed azo dye Congo Red on the biomass. Shifting and intensification of a strong peak from 2,924.17 to 2,921.93 cm^{-1} indicates –CH symmetric stretch of the methylene groups ($-CH_2$) and deformation vibration of methyl groups ($-CH_3$). The peak at

Table 5 Desorption of azo dye Congo Red onto free and immobilized *Trametes pubescens* biomasses in the optimal conditions

Biomass	Cycle	Adsorption capacity (mg/g)	Desorption capacity (mg/g)	Recovery (%)
Free	1	138.35	135.54	97.969
	2	127.54	122.31	95. 899
	3	114.21	105.84	92.671
Alginate-immobilized	1	548.47	534.14	97.387
	2	541.83	531.21	98.040
	3	536.41	505.58	94.252
D201-immobilized	1	265.58	258.82	97.455
	2	256.51	244.53	95.330
	3	245.84	229.10	93.191

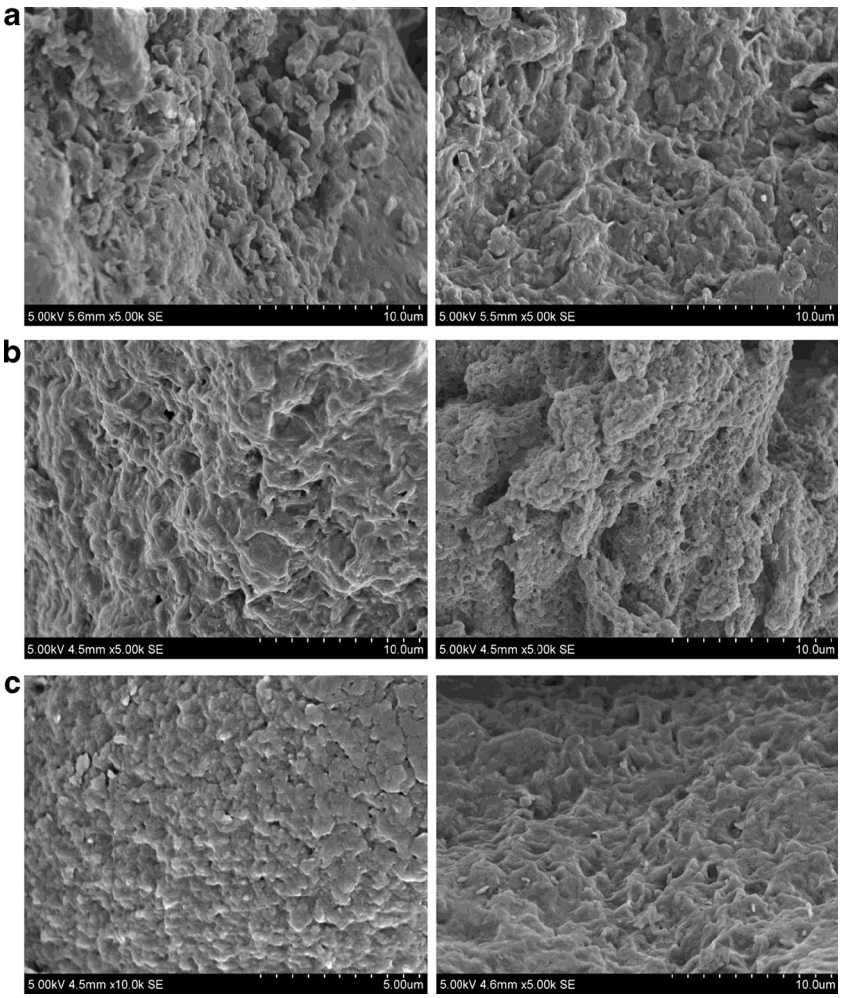

Fig. 2 SEM photomicrographs of free (**a**), alginate-immobilized (**b**), and D201-immobilized (**c**) *Trametes pubescens* biomasses before and after dye loading

1,628.59 cm^{-1} may be attributed to –C = O stretching vibration of carboxylate (−COO) or −NH deformation vibration of amide I groups. The spectrum of dye-loaded free biomass also indicates the intensity increase in the adsorption band near 1,380 cm^{-1} (from 1,376.24 to 1,396.89 cm^{-1}), corresponding to –CH bending, $-CH_3$ stretch, or –COO symmetric stretch. A peak at 1,020.74 cm^{-1} visible mainly on dye loaded biomass are due to the –C − O stretching vibration of ketones, aldehydes, and lactones or carboxyl groups. Thus, amide, hydroxyl, carboxylate, −C −O, methyl, and methylene groups seem to participate in adsorption of azo dye Congo Red on the surface of *T. pubescens* biomass, causing shifts in wave numbers, due to change in bonding energy in the corresponding functional groups (Kousha et al. 2012). In the spectrum of the alginate-immobilized *T. pubescens* biomass, the intensity of the peak at 2,923.52 cm^{-1} ascribed to $-CH_2$ stretching vibrations was weaker than that of the free biomass. It is also noted that peaks at 2,360.80 and 1,376.24 cm^{-1} for immobilized biomass disappeared. Peaks at 1,204.67 and 1,151.39 cm^{-1} may be attributed to a –C −N stretch of amide or amine of the biomass surface following immobilization with alginate. The FT-IR spectrum of the treated biomass exposed to Congo Red dye displayed a new peak at 1,453.42 cm^{-1}, which is due to the –CH deformations of $-CH_2$ or $-CH_3$ groups in aliphatics. Additionally, a new sharp band at 755.74 cm^{-1} is indicative of the involvement of −S = O group in dye adsorption. In the case of the D201-immobilized *T. pubescens* biomass after adsorption of Congo Red dye, the peak at 1,558.44 cm^{-1} was significantly shifted to 1,542.04 cm^{-1}, indicating the strong interaction of the dye with amide I and II functional groups. The band observed at 1,007.87 cm^{-1} shifting to 1,028.40 cm^{-1} is assigned to –C − O stretching vibration of alcohols and carboxylic acids.

X-ray diffraction technique is a powerful tool to analyze the crystalline nature of the materials. Adsorption reaction may lead to change in molecular and crystalline structure of the adsorbent and hence an understanding of the molecular structure and crystalline structure of the adsorbent, and the resulting changes thereof would provide valuable information regarding

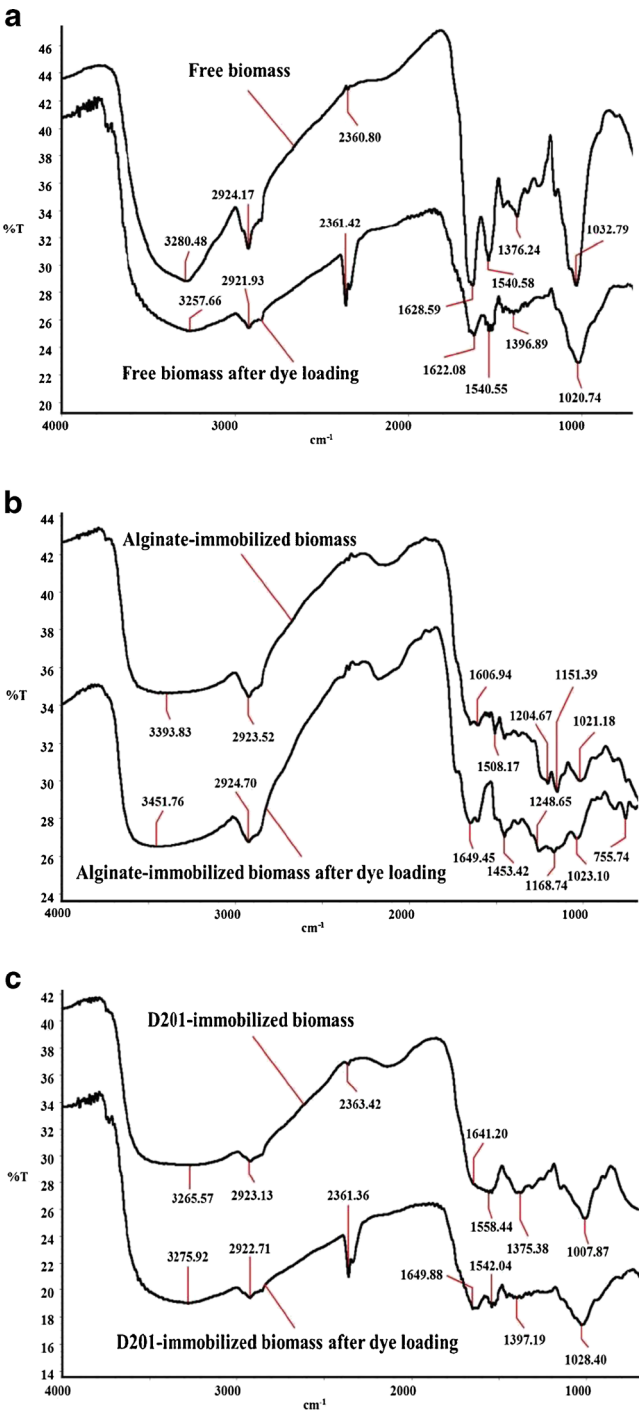

Fig. 3 FT-IR spectra of free (**a**), alginate-immobilized (**b**), and D201-immobilized (**c**) *Trametes pubescens* biomasses before and after dye loading

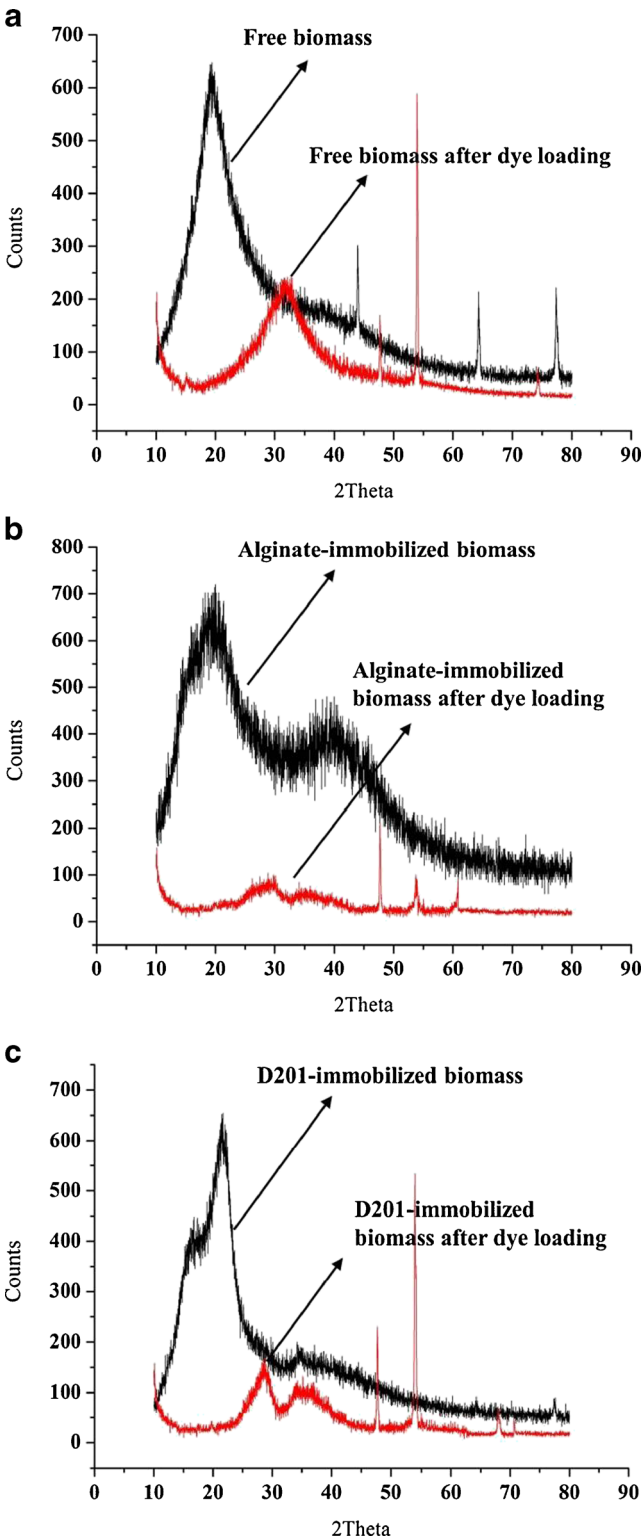

Fig. 4 X-ray diffractograms of free (**a**), alginate-immobilized (**b**), and D201-immobilized (**c**) *Trametes pubescens* biomasses before and after dye loading

adsorption reaction (Namasivayam and Kavitha 2006). As depicted in Fig. 4, it appears that the free and immobilized *T. pubescens* biomasses are crystalline in nature and show sharp peaks corresponding to 2θ= 19.44, 19.98, and 21.66, respectively. However, the XRD patterns of the dye-laden free and immobilized biomasses display typical amorphous characters, which suggest that the dye molecules diffuse into micropores and macropores and adsorb mostly by chemisorption with altering the structure of the biomass, as a result of the adsorption reaction.

Conclusion

Immobilization-treated biomass from white rot fungus *T. pubescens* was observed to adsorb azo dye Congo Red more efficiently than free biomass. Adsorption at lower pH enhanced the efficiency of dye removal. The presence of salt ions or increased ionic strength affected the dye sorption weakly. Dye adsorption process followed the pseudo-second-order kinetic and Freundlich isotherm models. The quantitative recovery of the dye can be achieved by treating dye-loaded biomass with 0.1 M NaOH. These findings suggested that the biomass produced by *T. pubescens* may be an alternative for removal of azo dyes from aqueous media.

Acknowledgments This study was supported by the Fundamental Research Funds for the Central Universities (No. JC2013-1) and Beijing Higher Education Young Elite Teacher Project (YETP0774).

References

Aksu Z (2005) Application of biosorption for the removal of organic pollutants: a review. Process Biochem 40:997–1026

Aksu Z, Balibek E (2010) Effect of salinity on metal-complex dye biosorption by *Rhizopus arrhizus*. J Environ Manag 91:1546–1555

Anjaneya O, Souche SY, Santoshkumar M, Karegoudar TB (2011) Decolorization of sulfonated azo dye Metanil Yellow by newly isolated bacterial strains: *Bacillus* sp. strain AK1 and *Lysinibacillus* sp. strain AK2. J Hazard Mater 190:351–358

Asgher M, Bhatti HN (2010) Mechanistic and kinetic evaluation of biosorption of reactive azo dyes by free, immobilized and chemically treated *Citrus sinensis* waste biomass. Ecol Eng 36:1660–1665

Bayramoğlu G, Çelik G, Arica MY (2006) Biosorption of Reactive Blue 4 dye by native and treated fungus *Phanerochaete chrysosporium*: batch and continuous flow system studies. J Hazard Mater 137:1689–1697

Bhattacharyya KG, Sharma A (2004) *Azadirachta indica* leaf powder as an effective biosorbent for dyes: a case study with aqueous Congo Red solutions. J Environ Manag 71:217–229

Binupriya A, Sathishkumar M, Swaminathan K, Kuz C, Yun S (2008) Comparative studies on removal of Congo Red by native and modified mycelial pellets of *Trametes versicolor* in various reactor modes. Bioresour Technol 99:1080–1088

Champagne PP, Ramsay JA (2010) Dye decolorization and detoxification by laccase immobilized on porous glass beads. Bioresour Technol 101:2230–2235

Çolak F, Atar N, Olgun A (2009) Biosorption of acidic dyes from aqueous solution by *Paenibacillus macerans*: kinetic, thermodynamic and equilibrium studies. Chem Eng J 150:122–130

Crini G, Peindy HN, Gimbert F, Robert C (2007) Removal of C.I. Basic Green 4 (Malachite Green) from aqueous solutions by adsorption using cyclodextrin-based adsorbent: kinetic and equilibrium studies. Sep Purif Technol 53:97–110

Dai YC (2012) Polypore diversity in China with an annotated checklist of Chinese polypores. Mycoscience 53:49–80

Daneshvar N, Ayazloo M, Khataee AR, Pourhassan M (2007) Biological decolorization of dye solution containing Malachite Green by microalgae *Cosmarium* sp. Bioresour Technol 98:1176–1182

Dawood S, Sen TK (2012) Removal of anionic dye Congo Red from aqueous solution by raw pine and acid-treated pine cone powder as adsorbent: equilibrium, thermodynamic, kinetics, mechanism and process design. Water Res 46:1933–1946

Dotto GL, Cadaval TRS, Pinto LAA (2012) Use of *Spirulina platensis* micro and nanoparticles for the removal synthetic dyes from aqueous solutions by biosorption. Process Biochem 47:1335–1343

Freundlich HMF (1906) Über die adsorption in lösungen. Z Phys Chem 57:385–470

Fu Y, Viraraghavan T (2001) Fungal decolorization of dye wastewaters: a review. Bioresour Technol 79:251–262

Fu Y, Viraraghavan T (2002) Removal of Congo Red from an aqueous solution by fungus *Aspergillus niger*. Adv Environ Res 7:239–247

Han R, Ding D, Xu Y, Zou W, Wang Y, Li Y, Zou L (2008) Use of rice husk for the adsorption of Congo Red from aqueous solution in column mode. Bioresour Technol 99:2938–2946

Hosseini Koupaie E, Alavi Moghaddam MR, Hashemi SH (2012) Investigation of decolorization kinetics and biodegradation of azo dye Acid Red 18 using sequential process of anaerobic sequencing batch reactor/moving bed sequencing batch biofilm reactor. Int Biodeterior Biodegrad 71:43–49

Khataee AR, Dehghan G, Ebadi A, Zarei M, Pourhassan M (2010) Biological treatment of a dye solution by Macroalgae *Chara* sp.: effect of operational parameters, intermediates identification and artificial neural network modeling. Bioresour Technol 101:2252–2258

Kousha M, Daneshvar E, Sohrabi MS, Jokar M, Bhatnagar A (2012) Adsorption of acid orange II dye by raw and chemically modified brown macroalga *Stoechospermum marginatum*. Chem Eng J 192:67–76

Mendes S, Farinha A, Ramos CG, Leitão JH, Viegas CA, Martins LO (2011) Synergistic action of azoreductase and laccase leads to maximal decolourization and detoxification of model dye-containing wastewaters. Bioresour Technol 102:9852–9859

Namasivayam C, Kavitha D (2006) IR, XRD and SEM studies on the mechanism of adsorption of dyes and phenols by coir pith carbon from aqueous phase. Microchem J 82:43–48

Oladoja NA, Akinlabi AK (2009) Congo Red biosorption on palm kernel seed coat. Ind Eng Chem Res 48:6188–6196

Panda GC, Das SK, Guha AK (2009) Jute stick powder as a potential biomass for the removal of congo red and rhodamine B from their aqueous solution. J Hazard Mater 164:374–379

Parshetti G, Kalme S, Saratale G, Govindwar S (2006) Biodegradation of malachite green by *Kocuria rosea* MTCC 1532. Acta Chim Slov 53:492–498

Pathak H, Patel S, Rathod M, Chauhan K (2011) In vitro studies on degradation of synthetic dye mixture by *Comamonas* sp. VS-MH2 and evaluation of its efficacy using simulated microcosm. Bioresour Technol 102:10391–10400

Shah PD, Dave SR, Rao MS (2012) Enzymatic degradation of textile dye Reactive Orange 13 by newly isolated bacterial strain *Alcaligenes faecalis* PMS-1. Int Biodeterior Biodegrad 69:41–50

Si J, Cui BK (2013) Dye Congo Red adsorptive decolorization by adsorbents obtained from *Trametes pubescens*. Desalin Water Treat 51:37–39

Si J, Peng F, Cui BK (2013a) Purification, biochemical characterization and dye decolorization capacity of an alkali-resistant and metal-tolerant laccase from *Trametes pubescens*. Bioresour Technol 128:49–57

Si J, Cui BK, Dai YC (2013b) Decolorization of chemically different dyes by white-rot fungi in submerged cultures. Ann Microbiol 63:1099–1108

Sun XF, Wang SG, Liu XW, Gong WX, Bao N, Ma Y (2008) The effects of pH and ionic strength on fulvic acid uptake by chitosan hydrogel beads. Colloids Surf A Physicochem Eng Asp 324:28–34

Vijayaraghavan K, Yun YS (2008) Bacterial biosorbents and biosorption. Biotechnol Adv 26:266–291

Wang L, Zhang J, Zhao R, Li C, Li Y, Zhang C (2010) Adsorption of basic dyes on activated carbon prepared from *Polygonum orientale*

Linn: equilibrium, kinetic and thermodynamic studies. Desalination 254:68–74

Xi Y, Shen YF, Yang F, Yang GJ, Liu C, Zhang Z, Zhu DH (2013) Removal of azo dye from aqueous solution by a new biosorbent prepared with *Aspergillus nidulans* cultured in tobacco wastewater. J Taiwan Inst Chem Eng 44:815–820

Xin B, Zhang Y, Liu C, Chen S, Wu B (2012) Comparison of specific adsorption capacity of different forms of fungal pellets for removal of Acid Brilliant Red B from aqueous solution and mechanisms exploration. Process Biochem 47: 1197–1201

Xiong XJ, Meng XJ, Zheng TL (2010) Biosorption of C.I. Direct Blue 199 from aqueous solution by nonviable *Aspergillus niger*. J Hazard Mater 175:241–246

Yang H, Feng Q (2010) Characterization of pore-expanded amino-functionalized mesoporous silicas directly synthesized with dimethyldecylamine and its application for decolorization of sulphonated azo dyes. J Hazard Mater 180:106–114

Yang Y, Wang G, Wang B, Li Z, Jia X, Zhou Q, Zhao Y (2011) Biosorption of Acid Black 172 and Congo Red from aqueous solution by nonviable *Penicillium* YW 01: kinetic study, equilibrium isotherm and artificial neural network modeling. Bioresour Technol 102:828–834

Zeng X, Cai Y, Liao X, Zeng X, Li W, Zhang D (2011) Decolorization of synthetic dyes by crude laccase from a newly isolated *Trametes trogii* strain cultivated on solid agro-industrial residue. J Hazard Mater 187:517–525

Zhang Z, Moghaddam L, O'Hara IM, Doherty WOS (2011) Congo Red adsorption by ball-milled sugarcane bagasse. Chem Eng J 178:122–128

Zhang J, Feng M, Jiang Y, Hu M, Li S, Zhai Q (2012) Efficient decolorization/degradation of aqueous azo dyes using buffered H_2O_2 oxidation catalyzed by a dosage below ppm level of chloroperoxidase. Chem Eng J 191:236–242